Impact of travel patterns on epidemic dynamics in heterogeneous spatial metapopulation networks

Shunjiang Ni[1,2,*] and Wenguo Weng[1]
[1]*Center for Public Safety Research, Department of Engineering Physics, Tsinghua University, Beijing, 100084, China*
[2]*School of Aerospace, Tsinghua University, Beijing, 100084, China*
(Received 18 August 2008; published 26 January 2009)

We report the results of a series of simulations of a susceptible-infected-recovered epidemic model in heterogeneous spatial metapopulation networks with quantitative knowledge of human traveling statistics that human travel behavior obeys scaling laws in the sense of geographical distance and period of waiting time. By tuning the edge length distribution of the spatial metapopulation network, we can conveniently control the distribution of human travel distance. The simulation results show that the occurrence probability of global outbreaks is significantly dependent on the characteristic travel distance, the characteristic waiting time, and the memory effects of human travel. We also present some preliminary results on the effects of travel restrictions in epidemic control.

DOI: 10.1103/PhysRevE.79.016111 PACS number(s): 89.75.Da, 89.75.Fb, 89.75.Hc, 89.65.−s

I. INTRODUCTION

The study of human activity patterns at different spatial and temporal scales has been paid much attention in recent years, such as the bursts and heavy tails in human dynamics [1–3], the evolution of human trail systems [4], and the scaling laws for the movement of people between locations in a large city [5]. Human activity is not only the driving force of many observed complex social phenomena, but also has significant impact on many related dynamical processes. For example, Vazquez *et al.* [6] investigated the impact of non-Poissonian human activity patterns on the email worm's spread and proved the failure of the Poisson approximation for the inter-event time distribution that is currently used in all epidemic models. In epidemiology, human travel has been treated as one of the important ingredients responsible for large-scale epidemic outbreaks [7–11]. These studies have mainly focused on the role of the large-scale properties of airline or railway transportation networks in global epidemics, where the human travel process has been oversimplified due to the lack of quantitative knowledge of human traveling statistics. Recently, Brockmann *et al.* [12] analyzed the dispersal of bank notes in the United States and extracted the scaling laws of human travel; i.e., the human travel distance r and the rest time t_w between displacements obey the heavy-tailed distributions $p(r)\sim r^{-(1+b)}$ and $p(t_w)\sim t_w^{-(1+a)}$, respectively, where they predicted $a=b=0.6$. Consequently, it has an important chance to help understand how human travel patterns affect the geographical spread of human infectious disease.

In modeling of the large-scale transmission of infectious disease, Watts *et al.* [13] concluded that the metapopulation models offer a potentially useful compromise between compartment models and networks, and they proposed a hierarchical metapopulation model to investigate the multiscale and resurgent epidemics in large populations. Colizza and Vespignani [14] introduced heterogeneous metapopulation networks with a simplified human travel scheme to analyze the large-scale spread of epidemics and found that the spreading dynamics was jointly determined by the mobility rate of individuals and the topology of the metapopulation network. These studies imply that the quantitative descriptions of more realistic human movement in geographical environment should be taken into account in epidemic spreading. In this paper we take the advantage of the spatial networks or geographical networks, which have been recently studied by several authors [15–17], to explicitly incorporate the geographical ingredient into our model. Specifically, we introduce a spatial matapopulation network to model the population structure. Each node of the spatial metapopulation network represents a subpopulation, and individuals can travel from one subpopulation to another subpopulation along the network links. The distribution of human travel distance can be regulated conveniently by adjusting the distribution of link length of the spatial metapopulation networks. In each subpopulation, we take the SIR epidemic model as a simple description of the local infection dynamics, which is coupled by the travel process. Through this paradigm, we intend to investigate the impact of the human travel pattern on the spreading process of infectious disease.

II. MODEL

In our model, the total population is divided into N subpopulations, each of which is represented by a node of the metapopulation network. We assume that each node i is initially occupied by N_i individuals and has the node degree k_i; i.e., the node i is connected to other k_i nodes. In this way, these subpopulations are connected by a network with degree distribution p_k and individuals can diffuse along the network links according to their travel pattern. In order to incorporate the scaling law of human travel into our model, we define the network substrate on a two-dimensional square space of unitary length on the x-y plane with periodic boundary conditions. Specifically, each node i $(i=1,2,\ldots,N)$ is randomly

*Author to whom correspondence should be addressed. nsj04@mails.tsinghua.edu.cn

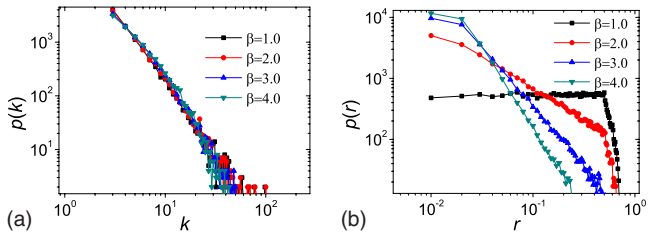

FIG. 1. (Color online) Degree (a) and edge length (b) distributions of the metapopulation network of $N=10^4$, $m=3$, $\alpha=1.0$, and $\beta=1.0$ (squares), 2.0 (circles), 3.0 (up triangles), and 4.0 (down triangles).

assigned a pair of values (x_i, y_i) to represent its coordinates on the geographical plane. We assume that each coordinate is an independent and identically distributed random number drawn within the interval [0,1). Initially, m fully connected nodes, labeled by $1,2,\ldots,m$, respectively, are randomly distributed in the square, and then at each time step t ($t=m+1$, $m+2,\ldots,N$), a new node labeled by t is added to the network and connected to m preexisting nodes according to the attachment probability that the node i ($i=1,2,\ldots,t-1$) would be chosen to connect to the newly added node t:

$$\pi_i(t) \sim k_i^{\alpha}(t)/d_{it}^{\beta}, \tag{1}$$

where d_{it} is the Euclidean distance between the nodes t and i, which is measured using periodic boundary conditions, and α and β are two tuning parameters governing the degree distribution, and link length distribution, respectively [16–18]. The degree distribution of the resulting network can be obtained by using mean-field theory [16,18] for $0 \leqslant \alpha < 1$ and finite β and is given by

$$p(k) = Am^{-1}k^{-\alpha}e^{-A(k^{1-\alpha}-m^{1-\alpha})/m(1-\alpha)}, \tag{2}$$

where A is a constant and can be determined by the requirement of the normalization [16]. For $\alpha=1$, mean-field theory yields the power-law degree distribution $p_k \sim k^{-3}$ [16]. However, for $\alpha>1$, an analytical solution is unavailable because most of the nodes are connected to a few number of nodes. Figure 1(a) illustrates the degree distributions for different parameters of β, which supports well the analytical results. The link length distribution, which is defined as the probability that a randomly selected link has the length r, is given by

$$p(r) \sim r^{-\beta+1}, \tag{3}$$

where $1 \leqslant \beta \leqslant 4$ and $0 \leqslant \alpha \leqslant 1$ [16,17]. Figure 1(b) illustrates the link length distributions, which are uniform for $\beta=1$ and heavy tailed for $\beta>1$, agreeing well with analytical predictions. It should be noted that the link length is measured under the periodic conditions; thus, it can reach at most $\sqrt{2}/2$, which also can be seen in Fig. 1(b).

Our purpose is to adopt the heavy-tailed distribution of the link length to model the scaling law of human travel distance. In the following sessions, we fix $\alpha=1.0$ to maintain the power-law degree distribution and vary β from 1.0 to 4.0 to tune the link length distribution. The human travel process is modeled as follows.

(i) *Traveling*. For each individual h initially located in node i, at each time step, it will leave node i with probability p_{jump} and enter into a node j that is randomly selected from the neighboring nodes of node i, then go to step (ii); otherwise, individual h will remain in the node i.

(ii) *Waiting*. When individual h enters into a node j, it will be assigned a waiting time t_w that is drawn from a heavy-tailed distribution $p(t_w) \sim t_w^{-(1+\lambda)}$, where $\lambda>0$ and $1 \leqslant t_w \leqslant T_{\max}$; then, the individual h will wait for t_w time steps in node j before it travels again.

(iii) *Returning*. After waiting for t_w time steps in node j, the individual h will return back to node i with probability p_{back}, then start from step (i) again at the next time step; otherwise, it will travel to another node k that is randomly selected from the neighboring nodes of node j, followed by step (ii).

The local infection dynamics within each node or subpopulation is described by a susceptible-infected-recovered (SIR) model [19]. In each node i, the subpopulation $N_i(t)$ at time t is constituted of three compartments: susceptible $[S_i(t)]$, infected $[I_i(t)]$, and recovered $[R_i(t)]$—i.e., $N_i(t) = S_i(t)+I_i(t)+R_i(t)$. In the current study, we assume that $N_i(t=0)=n$ for all nodes $i=1,2,\ldots,N$, where n is a constant. Then $N_i(t)$ will vary with time due to the travel process. The probability of being infected for each susceptible individual h in node i at time t is dependent on the number of infected individuals $I_i(t)$. Specifically, let p_{inf} be the probability that a susceptible individual will be infected due to its contact with exact one infected individual; then, each susceptible individual in node i will be infected with probability $p=1-(1-p_{\text{inf}})^{I_i}$, and after τ time steps, the newly infected individual will turn to the recovered individual permanently. The basic reproduction number, which is defined as the expected number of secondary cases generated by one primary case in a susceptible population, is simply given as $R_0=np_{\text{inf}}\tau$. The infection dynamics is started with one infective individual that is randomly selected from the total population and proceeds in parallel at each time step. For $R_0<1$, the local outbreak will die out quickly. For $R_0>1$ and large enough traveling probability p_{jump}, the initial infectious node may transmit the disease into other nodes.

III. RESULTS AND DISCUSSION

We have performed extensive numerical simulations of the metapopulation system without any exogenous interventions with the initial condition of a single infection that is randomly selected from the whole population. As a necessary condition, we have chosen $n=100$, $\tau=10$, and $p_{\text{inf}}=0.003$ such that $R_0=3$ in order to ensure that epidemics of some nontrivial size occur with nonzero probability. Figures 2(a)–2(d) show four example time series of newly infected cases with the same configuration of model parameters, where the spreading processes display two striking features: (i) the epidemics that succeed in breaking out from their initial subpopulations either die out quickly before invading their neighboring subpopulations [Fig. 2(a)] or infect a number of other subpopulations [Figs. 2(b)–2(d)]; (ii) for nonlocal epidemics [Figs. 2(b)–2(d)], the infection curves exhibit

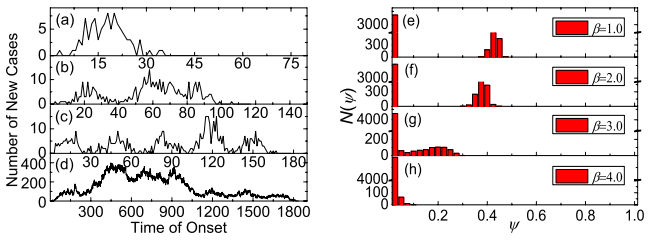

FIG. 2. (Color online) (a)–(d) Example time series of newly infected cases, where, in all cases, simulation parameters are $N=10^4$, $m=3$, $n=100$, $\alpha=1.0$, $\beta=2.6$, $\lambda=0.6$, $p_{\text{jump}}=0.001$, $p_{\text{back}}=1.0$, $p_{\text{inf}}=0.003$, $T_{\max}=365$, and $\tau=10$. (e)–(h) The epidemic size distributions generated from 5000 simulations of the model for different values of $\beta=1.0$ (e), 2.0 (f), 3.0 (g), and 4.0 (h), where in all cases, the other parameters are the same as those in (a)–(d).

stochastic fluctuations at the level of individuals and subpopulations and have different durations, which can be characterized as the resurgence property [13]. In Figs. 2(e)–2(h), we plot the bimodal distributions of epidemic size ψ that is defined as the infection fraction during an epidemic for different values of β, from which we can see that the epidemic size distributions tend toward a single peak near $\psi=0$ as β increases, corresponding to a decreasing global invasion probability.

Figure 3 shows the average profiles that display the evolution of the cumulative infected persons over time for different parameter values of β and λ. It is observed that the propagation velocity and the peak value of the cumulative cases greatly decrease as the increasing β and λ. However, larger β and λ also prolong the epidemic persistence of the infectious diseases.

In order to investigate the impact of travel distance distribution on the infection spreading, we measure the survival probability $P(\psi>\psi_c)$, which is defined as the fraction of simulations that the epidemic size ψ is greater than a critical value ψ_c and the expected epidemic size $\langle\psi\rangle$ versus the exponent β of the travel distance distribution, as shown in Fig. 4(a). The curves are very similar in shape; i.e., they all decrease smoothly as the increasing β. This result can be explained as follows. According to Fig. 1(b), the increase of β results in fewer long-range connections between nodes

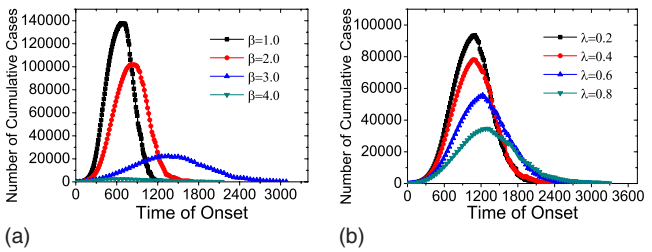

FIG. 3. (Color online) Evolution of the cumulative number of infected persons over time that averaged over 1000 simulations for different parameter values of β and λ. (a) $\beta=1.0$ (squares), 2.0 (circles), 3.0 (triangles up), 4.0 (triangles down), and $\lambda=0.6$. (b) $\lambda=0.2$ (squares), 0.4 (circles), 0.6 (triangles up), 0.8 (triangles down), and $\beta=2.6$. The other parameters for both (a) and (b) are $N=10^4$, $m=3$, $n=100$, $\alpha=1.0$, $p_{\text{jump}}=0.001$, $p_{\text{back}}=1.0$, $p_{\text{inf}}=0.003$, $T_{\max}=365$, and $\tau=10$.

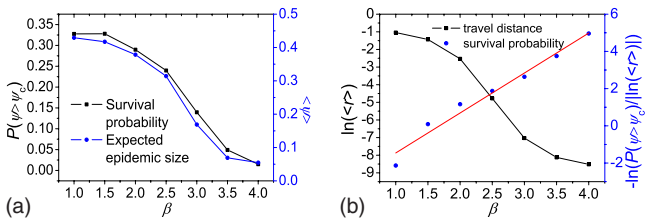

FIG. 4. (Color online) (a) Survival probability $P(\psi>\psi_c)$ (squares) and the corresponding expected epidemic size $\langle\psi\rangle$ (circles) versus the exponent β, where $\psi_c=0.025$ and $\langle\psi\rangle$ is averaged over all $\psi>\psi_c$. Each point is generated from 5000 simulations of the model, with simulation parameters $N=10^4$, $m=3$, $n=100$, $\alpha=1.0$, $\lambda=0.6$, $p_{\text{jump}}=0.001$, $p_{\text{back}}=1.0$, $p_{\text{inf}}=0.003$, $T_{\max}=365$, and $\tau=10$. (b) Curves for the rescaled characteristic travel distance $\langle r\rangle$ (squares) and the rescaled survival probability $\ln[P(\psi>\psi_c)/|\ln(\langle r\rangle)|]$ (circles) versus β. Here, $\langle r\rangle$ is given by Eq. (4).

(subpopulations), which restricts the scope of human travel to protect the network from epidemic spreading. For the travel distance distribution $p(r)\sim r^{-(1+\gamma)}$ $(-1\leqslant\gamma\leqslant 2)$, we can calculate the characteristic travel distance $\langle r\rangle$ as follows:

$$\langle r\rangle = \int_{r_{\min}}^{r_{\max}} p(r) r dr$$

$$= \begin{cases} \dfrac{\gamma}{1-\gamma}\dfrac{r_{\max}^{1-\gamma}-r_{\min}^{1-\gamma}}{r_{\min}^{-\gamma}-r_{\max}^{-\gamma}}, & -1\leqslant\gamma\leqslant 2 \text{ and } \gamma\neq 0,1, \\ (r_{\max}-r_{\min})/\ln\dfrac{r_{\max}}{r_{\min}}, & \gamma=0, \\ \dfrac{1}{r_{\min}^{-1}-r_{\max}^{-1}}\ln\dfrac{r_{\max}}{r_{\min}}, & \gamma=1, \end{cases} \tag{4}$$

where $\gamma=\beta-2$, $r_{\max}=\sqrt{2}/2$, and $r_{\min}=1/N$ is the mean minimum distance between nodes and treated as a constant determined only by the system size N. Figure 4(b) shows the curve of $\ln\langle r\rangle$ versus β, which is similar in shape as the curve of $P(\psi>\psi_c)$ versus β in Fig. 4(a). This result indicates that there is some positive relevance between the survival probability and the characteristic travel distance. In Fig. 4(b) we depict the rescaled survival probability as a function of β, which exhibits a linear dependence and can be expressed as the empirical formula $P(\psi>\psi_c)\sim e^{-\beta}\ln(\langle r\rangle)$. In [14], the authors declared that the global survival probability is mainly determined by the basic reproductive number R_0, the mobility rate p_{jump}, and the network heterogeneity. Here, our results demonstrate that the spatial mode of human travel is also an important factor for epidemic spreading.

Figure 5(a) reports the behavior of the survival probability $P(\psi>\psi_c)$ as a function of the exponent λ of the waiting time distribution with two different maximal waiting time $T_{\max}$. The curves show an initial increase, reach the peak at $\lambda\approx 0.3$ for $T_{\max}=365$ and $\lambda\approx 0.4$ for $T_{\max}=730$, respectively, and then decrease linearly as λ increases. Similarly, we plot the rescaled characteristic waiting time $\langle t_w\rangle/\tau$ as well as the rescaled survival probability $P(\psi>\psi_c)/(\langle t_w\rangle/\tau)$ versus the exponent λ, where $\langle t_w\rangle=\int_1^{T_{\max}} p(t_w) t_w dt_w$, as shown in Fig.

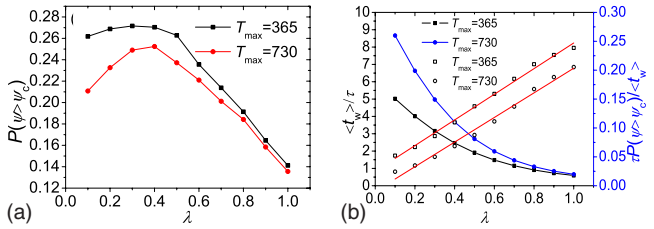

FIG. 5. (Color online) (a) Survival probability $P(\psi>\psi_c)$ as a function of λ for maximal waiting time $T_{max}=365$ (squares) and 730 (circles), where $\psi_c=0.025$. Each point is generated from 5000 simulations of the model, with simulation parameters $N=10^4$, $m=3$, $n=100$, $\alpha=1.0$, $\beta=2.6$, $p_{jump}=0.001$, $p_{back}=1.0$, $p_{inf}=0.003$, and $\tau=10$. (b) Curves for the rescaled mean waiting time $\langle t_w\rangle/\tau$ (solid squares for $T_{max}=365$ and solid circles for $T_{max}=730$) and the rescaled survival probability $P(\psi>\psi_c)/(\langle t_w\rangle/\tau)$ (open squares for $T_{max}=365$ and open circles for $T_{max}=730$) versus λ.

5(b). It can be noticed that $P(\psi>\psi_c)$ reaches the peak when $\langle t_w\rangle$ is much larger than the infective period τ—i.e., at $\langle t_w\rangle/\tau\approx 3$ or more. Another noteworthy phenomenon is that the rescaled survival probability $P(\psi>\psi_c)/(\langle t_w\rangle/\tau)$ is linearly dependent on the exponent λ, which leads to $P(\psi>\psi_c)\sim\lambda\langle t_w\rangle/\tau$.

In most previous studies, the human mobility process is based on the Markovian assumption that at each time step all individuals can travel with the same traveling probability without having memory of their origin. This assumption is clearly refuted by our daily experience. In the real world, individuals usually return to their original dwelling places after they have visited a number of destinations. This can be an effective mechanism to limit the scope of activities of individuals during a certain fixed time duration in order to reduce the risk of the epidemic spreading. For this reason, we consider the memory effects of individuals—that, once the individuals travel, they will return to the place of residence with probability p_{back}. The simulation result is shown in Fig. 6, where the survival probability grows approximately linearly as the return probability decreases—i.e., $P(\psi>\psi_c)\sim(1-p_{back})$. This result confirms that it is not appropriate to apply the Markovian assumption to the human travel process in models of epidemic spreading. For example, the survival

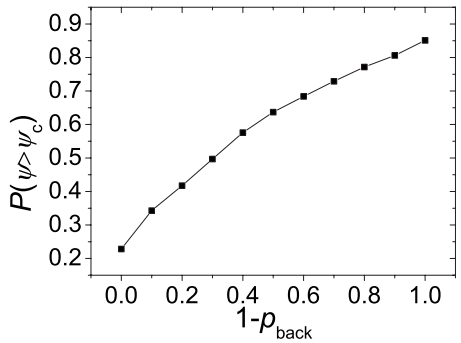

FIG. 6. Survival probability $P(\psi>\psi_c)$ as a function of p_{back}, where $\psi_c=0.025$. Each point is generated from 5000 simulations of the model, with simulation parameters $N=10^4$, $m=3$, $n=100$, $\alpha=1.0$, $\beta=2.6$, $\lambda=0.6$, $p_{jump}=0.001$, $p_{inf}=0.003$, $T_{max}=365$, and $\tau=10$.

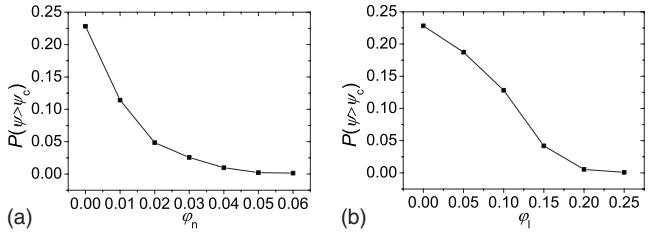

FIG. 7. Effects of the epidemic control strategies on the survival probability $P(\psi>\psi_c)$ where $\psi_c=0.025$. (a) Close $N\varphi_n$ largest degree nodes. (b) Shut off $Nm\varphi_l$ longest edges. Each point is generated from 5000 simulations of the model, with simulation parameters $N=10^4$, $m=3$, $n=100$, $\alpha=1.0$, $\beta=2.6$, $\lambda=0.6$, $p_{jump}=0.001$, $p_{inf}=0.003$, $p_{back}=1.0$, $T_{max}=365$, and $\tau=10$.

probability at $p_{back}=0$ corresponds to the case of the Markovian assumption, which is obviously overestimated compared to the case of $p_{back}>0$.

Finally, we have focused on the strategies for mitigating the effect of contagious disease outbreaks. Many nonpharmaceutical measures, such as case isolation, household quarantine, exit and entry screening, contact tracing, and travel restrictions, have been considered the commonly used prevention and containment strategies in the event of an epidemic or pandemic [7,20–23]. However, these measures can inflict significant negative impact on social and economic systems, and some of them are still controversial. So it is important to evaluate the effect of these measures on the spatial and temporal spread of contagious diseases, especially when the early recognition of the virus is ineffective. In the current work, we have investigated two control strategies, respectively: close $N\varphi_n$ largest degree nodes and shut off $Nm\varphi_l$ longest edges. The former corresponds to the closure of schools, workplaces, etc., and the latter corresponds to travel restrictions. According to Figs. 4–6, implementation of these two strategies is beneficial for epidemic control since it can restrict the scope of human travel. Figure 7 shows that $P(\psi>\psi_c)$ is markedly decreasing with the increasing φ_n and φ_l. For example, when $\varphi_n>0.03$ or $\varphi_l>0.15$ the survival probability $P(\psi>\psi_c)$ will be reduced to below 0.025. It is concluded that both strategies have significant influence on the epidemic spreading, which proves the effectiveness of the practical measures for epidemic spreading—i.e., school or workplace closure and travel restrictions in dealing with SARS [24–28].

In order to compare the above two control strategies, we consider the average distance on edges that emanate from a node i with degree k_i

$$d_i(k_i)=\frac{1}{k_i}\sum_{j\in\Upsilon} d_{ij}, \tag{5}$$

where d_{ij} is the distance on the edge that connects node i and j, and Υ represents the neighborhood of node i. The spatial metapopulation network gives rise to positive correlation between the degree of node and the average edge distance to its neighbors, as shown in Fig. 8. This result indicates that closing high-degree nodes and shutting off long-distance edges

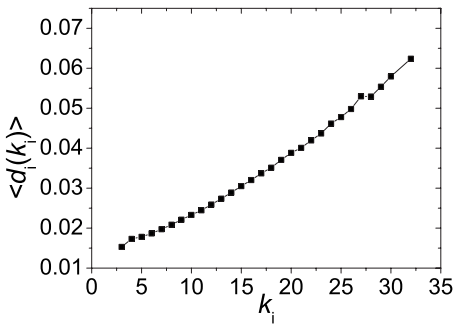

FIG. 8. Correlation between degree k and average distance $d(k)$ on edges of nodes with degree k. Results are averaged over 100 independent realizations of the network with $N=10^4$, $m=3$, $\alpha=1.0$, and $\beta=2.6$.

have actually more or less the same effects on epidemic spreading.

IV. CONCLUSIONS

The objective of this research is to set up a practical framework to explore the effects of human travel patterns on the spatiotemporal dynamics of large-scale epidemics. We introduce a heterogeneous spatial metapopulation network model, which is inspired by the spatial network model and the metapopulation model to represent the dynamical population structure due to the human travel process, where the travel distance and the waiting time between displacements obey heavy-tailed distributions and the effects of the memory of their origin have been considered. Each node of the spatial metapopulation network represents a subpopulation, and the degree distribution of the network can be tuned to be power law or exponential. The edge length obeys the heavy-tailed distribution, which is used to represent the distribution of human travel distance. In each subpopulation, we take the SIR model as a simple description of the local infection dynamics.

We then perform extensive numerical simulations of the above model and measure the survival probability and expected epidemic size for different configuration of the human travel patterns. We obtain the empirical relationships between the survival probability and the distribution of travel distance and the waiting time, as well as the memory effect. The results show that the occurrence probability of global outbreaks or the survival probability is significantly dependent on the characteristic travel distance, the characteristic waiting time, and the memory effects of human travel.

Finally, we present some preliminary simulation results of the epidemic control strategies. Two strategies have been investigated, i.e., closing a fraction of the largest degree nodes and shutting off some longest edges. Results show that both strategies are equally effective in inhibiting the spread of infectious diseases.

ACKNOWLEDGMENTS

The authors deeply appreciate support for this paper by the National Natural Science Foundation of China (Grant No. 70871069).

[1] A. L. Barabasi, Nature (London) **435**, 207 (2005).
[2] J. G. Oliveira and A. L. Barabasi, Nature (London) **437**, 1251 (2005).
[3] A. Vazquez, J. G. Olive, Z. Dezso, K. I. Goh, I. Kondor, and A. L. Barabasi, Phys. Rev. E **73**, 036127 (2006).
[4] D. Helbing, J. Keltsch, and P. Molnar, Nature (London) **388**, 47 (1997).
[5] G. Chowell, J. M. Hyman, S. Eubank, and C. Castillo-Chavez, Phys. Rev. E **68**, 066102 (2003).
[6] A. Vazquez, B. Racz, A. Lukacs, and A. L. Barabasi, Phys. Rev. Lett. **98**, 158702 (2007).
[7] M. Camitz and F. Liljeros, Bmc. Med. **4**, 32 (2006).
[8] R. F. Grais, J. H. Ellis, and G. E. Glass, Eur. J. Epidemiol. **18**, 1065 (2003).
[9] V. Colizza *et al.*, PLoS Med. **4**, 95 (2007).
[10] V. Colizza *et al.*, Proc. Natl. Acad. Sci. U.S.A. **103**, 2015 (2006).
[11] L. Hufnagel, D. Brockmann, and T. Geisel, Proc. Natl. Acad. Sci. U.S.A. **101**, 15124 (2004).
[12] D. Brockmann, L. Hufnagel, and T. Geisel, Nature (London) **439**, 462 (2006).
[13] D. J. Watts *et al.*, Proc. Natl. Acad. Sci. U.S.A. **102**, 11157 (2005).
[14] V. Colizza and A. Vespignani, Phys. Rev. Lett. **99**, 148701 (2007).
[15] G. Mukherjee and S. S. Manna, Phys. Rev. E **74**, 036111 (2006).
[16] Y. B. Xie, T. Zhou, W. J. Bai, G. Chen, W. K. Xiao, and B. H. Wang, Phys. Rev. E **75**, 036106 (2007).
[17] S. S. Manna and P. Sen, Phys. Rev. E **66**, 066114 (2002).
[18] X. J. Xu, X. Zhang, and J. F. F. Mendes, Phys. Rev. E **76**, 056109 (2007).
[19] M. Frasca, A. Buscarino, A. Rizzo, L. Fortuna, and S. Boccaletti, Phys. Rev. E **74**, 036110 (2006).
[20] R. F. Grais, J. H. Ellis, and G. E. Glass, Epidemiol. Infect. **131**, 849 (2003).
[21] J. Arino, R. Jordan, and P. van den Driessche, Math. Biosci. **206**, 46 (2007).
[22] N. M. Ferguson *et al.*, Nature (London) **442**, 448 (2006).
[23] T. D. Hollingsworth, N. M. Ferguson, and R. M. Anderson, Nat. Med. **12**, 497 (2006).
[24] L. James *et al.*, Public Health **120**, 20 (2006).
[25] Y. H. Hsieh *et al.*, Emerg. Infect. Dis. **11**, 278 (2005).
[26] C. C. Tan, Ann. Acad. Med. Singapore **35**, 345 (2006).
[27] K. T. Chen *et al.*, Int. J. Infect. Dis. **9**, 77 (2005).
[28] W. N. Liang *et al.*, Emerg. Infect. Dis. **10**, 25 (2004).